Crimson Publishers
Wings to the Research

Research Article

Catalytic Activity of Porous Crystalline Aluminosilicates in Continuous Nitrate Removal via Electroreduction

Ahmed Enmili[1]*, Frédéric Monette[1], Nasreddine Bendib[1], Abdelkrim Azzouz[1,2]*

[1]École de technologie supérieure, Montréal (Québec) H3C 1K3, Canada

[2]Université du Québec à Montréal, Montréal (Québec) H3C 3P8, Canada

ISSN: 2576-8840

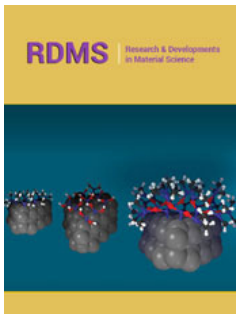

***Corresponding author:** Abdelkrim Azzouz, École de Technologie Supérieure, Montréal (Québec) H3C 1K3, Canada

Submission: November 21, 2023
Published: November 29, 2023

Volume 19 - Issue 4

How to cite this article: Ahmed Enmili*, Frédéric Monette, Nasreddine Bendib, Abdelkrim Azzouz*. Catalytic Activity of Porous Crystalline Aluminosilicates in Continuous Nitrate Removal via Electroreduction. Res Dev Material Sci. 19(4). RDMS. 000970. 2023.
DOI: 10.31031/RDMS.2023.19.000970

Abstract

Nitrate removal through electroreduction using stainless steel electrodes in recycle mode was found to be enhanced by addition of salts (NaCl, KCl, $NaCl_2$ and $MgCl_2$), acids (HCL, H_2SO_4; CH_3-COOH and H_3PO_4) or aluminosilicate-based catalysts (bentonite, kaolin, illite-montmorillonite mixture and clinoptilolite). High nitrate removal yields were obtained in the presence of salts under optimum flowrate. The ionic strength and current density induced by chlorinated salts appear to promote the electrochemical denitrification. This effect was stronger as compared to that produced by acid addition. Acid addition appears to mainly improve the ionic force. The flowrate effect was found to strongly correlate to those of all added species. These results open promising prospects for low-cost clay-catalyzed nitrate electroreduction under dynamic conditions.

Keywords: Nitrate; Clay minerals; Zeolites; Catalysts; Electroreduction

Introduction

Nitrate excess in nature mainly originate from anthropogenic activities reflected by in urban, industrial or agricultural and agro-industrial wastewaters [1-3]. Nitrates are essential plant growth, but their excessive occurrence in nature causes water eutrophication more particularly in lakes and rivers. This has become a major environmental issue that often results in uncontrolled algae spread with negative impacts not only on aquatic biodiversity [1,4] but also on human health, causing methemoglobinemia in infants [5], stomach cancer, colorectal cancer and non-Hodgkin's Lymphoma in adults [6].

Ample literature already reported more or less successful attempts targeting nitrate removal or reduction in waters. Many biological methods have been tested in this regard [7], revealing major shortcomings [8]. Physico-chemical techniques such as reverse osmosis resin ion exchange [9], coagulation and flocculation [10] turned out to be more effective in most cases, but the use of chemicals and production of undesired sludges are significant drawbacks that limit their large-scale implementation [11]. This has stimulated interest towards more eco-friendly routes that can process high nitrate concentrations with relatively low investment costs. Among these, nitrate electro-reduction is undoubtedly the most interesting alternative in this regard, more particularly when efficiently optimized for reducing the energy consumption or in the presence of nonpolluting and recyclable clay-based catalysts [12,13]. This process involves mainly cathodic reactions (Reactions 1-6) that convert nitrate anion into undesirable by-products such as nitrite and ammonia, but ultimalately into harmless nitrogen gas under optimal conditions [14].

$$NO_3^- + H_2O + 2e \leftrightarrow NO_2^- + 2OH^- \quad E^0 = 0{,}01\ V\ (1)$$

$$NO_3^- + 3H_2O + 5e \leftrightarrow \frac{1}{2}N_2 + 6OH^- \quad E^0 = 0{,}26\ V\ (2)$$

$$NO_3^- + 6H_2O + 8e \leftrightarrow NH_3 + 9OH^- \quad E^0 = -0{,}12\ V\ (3)$$

$$NO_2^- + 2H_2O + 3e \leftrightarrow \frac{1}{2}N_2 + 4OH^- \quad E^0 = 0{,}406\ V$$

$$NO_2^- + 5H_2O + 4e \leftrightarrow NH_2OH + 5OH^- \quad E^0 = -0{,}165\ V$$

$$NO_2^- + 4H_2O + 4e \leftrightarrow NH_2OH + 5OH^- \quad E^0 = -0,45\ V$$

Nitrate reduction mechanisms are strongly dependent on the medium pH, applied potential, electrode material, catalyst and design of the electrode-catalyst system [15,16]. Many research approaches have been tackled in order to investigate the influence of these parameters, targeting highly selective nitrate electroreduction into nitrogen [17]. Among various metals such as Cu [18], Sn [19], Ni [20], Ti [16,21], Fe [22], and Pb [23] tested as electrode materials, Cu cathodes turned out to be effective in nitrate electroreduction [18].

However, the general tendency is that combined metals such as Cu-Sn [24], Cu-Ni [16,25], Rh-Ni [18], Sn-Pd [21], Pt-Ir [26], Ag- Pd [22], Ag-Pt-Pd [22], Pd-Co-Cu alloy [27] and stainless steel [12,13] show higher activity and selectivity as compared to monometallic electrodes. Indeed, stainless steel electrodes allowed achieving nitrate removal yield exceeding 90% [12,13]. Pd/Cu electrodes with 15% Cu content showed significant activity and selectivity in the formation of ammonia [28]. Here, the Cu content and dispersion appears to play a key-role, since increasing Cu layer thickness was found to enhance the catalytic activity but at the expense of the selectivity.

The most recent trend in electrode design resides conferring an additional contribution of a catalytic property in nitrate electroreduction. So far, many attempts have been achieved through metal combination with catalytic materials in the presence of acids in different reactor configurations. The use of acids can be justified by the compensation of the unavoidable production of detrimental alkalinity that favorably shift equilibrium towards nitrate depletion (Reactions 6). However, acidic pH may also influence not only nitrate electroreduction [13,15] but also further protonation of the unavoidably generated ammonia and electro-conversion of free ammonium cation at the anode surface [29,30].

Microporous Aluminosilicates (AS) are expected to act as electrodes due to surface charge-induced electro-conductivity and as bifunctional catalysts that induce beneficial moderate acidity and surface activity. This was explained in terms of buffering effects of the solid surface and acidic species in the aqueous media, as reported earlier [13,31]. Here, the AS surface should act as a trap for the NH_4^+ cation resulting from the protonation of the generated ammoinia. This is supposed to simultaneously shift equilibrium towards enhanced nitration depletion and promote the electro-conversion in both adsorbed ammonium and small to trace amounts of released cations in the liquid phase nearly the anode [32-35]. This complex process is favored by decreasing pH, but excessively acidic media can cause detrimental electrocatalyst dealumination, more particularly below pH 2-3. Natural AS such as cationic clay minerals and some zeolites like clinoptilolites are interesting low-cost electrocatalysts that already showed effectiveness in nitrate and ammonium electro conversion in batch experiments [13,31].

Given that the design of the electrochemical cell and hydrodynamic regime were already found to strongly influence nitrate electroreduction process [16] and that studies on these processes under dynamic condition have barely been tackled, a special interest was herein devoted to investigate the catalytic activity of four AS. Thus, three clay materials such as kaolin, bentonite, illite + montmorillonite mixture and a zeolite (clinoptilolite) were selected for their different pH-dependent behaviors, chemical compositions, structures, and cation exchange capacity. The roles of the charge compensating cation and presence of various salts and acids were also examined in the process of nitrate electroreduction using stainless steel electrodes in recycle mode to reduce the negative effect of the dead volume. To reduce the effect of the dead volume, the perocess was performed in recycle mode. The process efficiency was discussed in correlation with the effects of the flow rate of the reaction mixture, ionic strength, and structural properties of the catalysts. The expected results should open promising prospects for using soils, sludges and natural clay-induced water turbidity as potential electrocatalyst for this purpose.

Materials and Methods

Materials characterization

Attempts to nitrate electroreduction were carried out by means of AISI-1018 stainless steel-based electrodes. Energy dispersive X–ray fluorescence (ED-XRF) measurements (Brücker Quantax 400 EDS) revealed the following chemical composition: C: 0.14 % - 0.20 %, Fe: 98.81 % - 99.26 % Mn: 0.60 % - 0.90 %, P ≤ 0.040 %, S ≤ 0.050 %).

Crude bentonite (SiO_2/Al_2O_3 = 2.98 w/w) containing 84% montmorillonite, illite (SiO_2/Al_2O_3 = 2.17 w/w) and kaolin (SiO_2/Al_2O_3 = 1.28 w/w) purchased from Aldrich were employed as clay electrodes in nitrate electroreduction attempts. Bentonite purification was not required, since crude bentonite and montmorillonite (96% purity) obtained through bentonite purification showed almost similar catalytic performances [13]. However, for the sake of rigor, bentonite performance was compared to that of its synthetic counterpart based on a 1:1 wt/wt illite-montmorillonite mixture, illite being another major impurity in bentonite. This comparative study was completed by clinoptilolite denoted as Clino (SiO_2/Al_2O_3 = 5.45 w/w), a zeolite-type catalyst. Further, 0.1-0.3mm grains of AS previously stored overnight under dry air in sealed enclosure at room temperature RT) were characterized through X-ray diffraction (XRD) using a Siemens D5000 equipment (Co-Kα at 1.7890Å). The same characterization data as previously obtained were discussed herein [13,31].

Nitrate electrochemical reduction

Nitrate source was provided $NaNO_3$ (Certified A.C.S. Crystal, CAS: 7631-99-4; 99.4 % purity, Fischer Scientific). Nitrate electroreduction experiments were performed at a current range of 0-5A provided by an ABRA DC power supply SPS-AB-D in a 1000mL cylindrical electrochemical cell acting as a batch reactor in recycle mode for reducing the negative effect of the dead volume outside the inter-electrode space. The device was equipped with eight stainless steel electrodes (Electrodes dimensions: 5cm x 5cm x 0.2cm) completely immersed by the nitrate solution (Figure S1). Preliminary experiments and previous works allowed setting an optimum inter-electrode distance of 4mm [12,13]. The influence of the flowrate on the process was assessed through a series of experiments carried out at various flow rates (1, 10, 20, 57, 67,

87 and 96mL·s^{-1}). The recycle mode was achieved with periodical assessment of nitrate concentration after each cycle by coupling the reactor to a peristaltic pump (50 cycles.min^{-1}) with controlled throughput by two 50cm length pipes with 1cm diameter. The overall volume in the recycle circuit was estimated as being of ca. 80mL, based on additional 2cm length pump hose. The initial pH was measured before connecting the electrode to the electric generator at a voltage ranging from 2 to 5V.

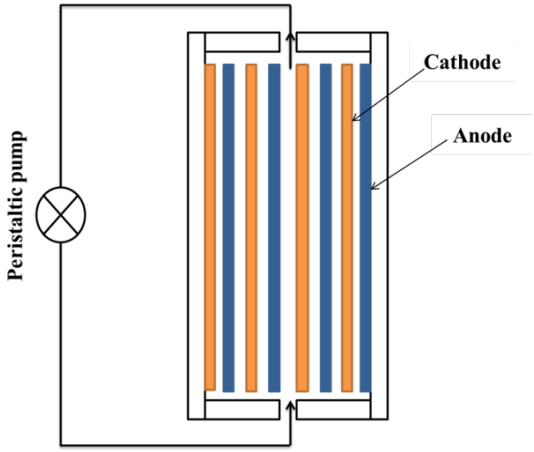

Figure S1: Schematic representation of the multi-cell Electrolyser.
Distance between electrodes: 4mm; Electrodes surface: 5cm x 5cm.

The influence of the catalyst type was examined by dispersing 0.2 g·L^{-1} of dry aluminosilicate in the same volume of the nitrate solution at intrinsic pH. The effect of the cation effect was investigated by adding 1g of salt to 1L of aqueous solution of nitrate anion at intrinsic pH, prepared by dissolving 1.37g of $NaNO_3$ in 1L of tap water. For this purpose, (from Merck, 99% purity), (from Fisher scientific, 99% purity), $CaCl_2 \cdot 2H_2O$ (from Anachemia, 99%) and $MgCl_2 \cdot 6H_2O$ (from VWR, 98%) were employed. Deeper insights in the role of the acid strength were achieved using various acids such as HCl (Anachemia, 37% purity), H_2SO_4 (Fisher chemical, 98%); CH_3- (VWR, 99%) and H_3PO_4 (Anachemia, 98%).

Analyses and measurements

Each of the successive 10mL samples (1% of the quantity of the reaction mixture) taken every 20min for 2h electroreduction process was diluted fifty times in order to obtain sufficient amounts for triplicate measurements of the residual nitrate concentration and alkalinity. The concentration of nitrate was measured through UV-Vis spectroscopy at a 220nm wavelength (Cary 300 Bio UV-visible spectrophotometer) using a standard method fully described elsewhere [36]. The main error in the conversion yield calculation in terms of mg-N·L^{-1} (ppm), arises from the UV-Vis measurement accuracy (±0.1mg-N·L^{-1}), and did not exceed 1.5% in all experiments. The pH of the solution was periodically determine using an OAKTON pH/conductivity/TDS/°C/°F meter, pH/CON 510 series device and the method N° 2320 Part B and Part B N° 2310 Section 4b (APHA, AWWA and WEF, 1995).

Results and Discussion

Flowrate effect on non-catalytic electroreduction

In recycle mode, nitrate concentration was found to decrease from ca. 960ppm down to approximately 588ppm for 1mL·s^{-1} but only to 615-616ppm for a much higher flowrate of 96mL·s^{-1} after 120min reaction time (Figure 1). The lowest residual nitrate concentration (464ppm) was registered for an intermediate 67mL·s^{-1} flowrate, after 120min in recycle mode, i.e. after 6030 cycles of the peristaltic pump. This suggests the occurrence of an optimum flowrate that produces an improve of the process as compared to the static mode where nitrate concentration remains relatively higher (485ppm). Quick optimization using a 3^2-factorial design of experiments [12,37-44] by centring the flowrate in the most probable range 25-70mL·s^{-1}, given the 1.5% accuracy in nitrate titration, and the process duration in the range 20-120min gave a calculated optimum flowrate of ca. 37± 5mL.min^{-1}.

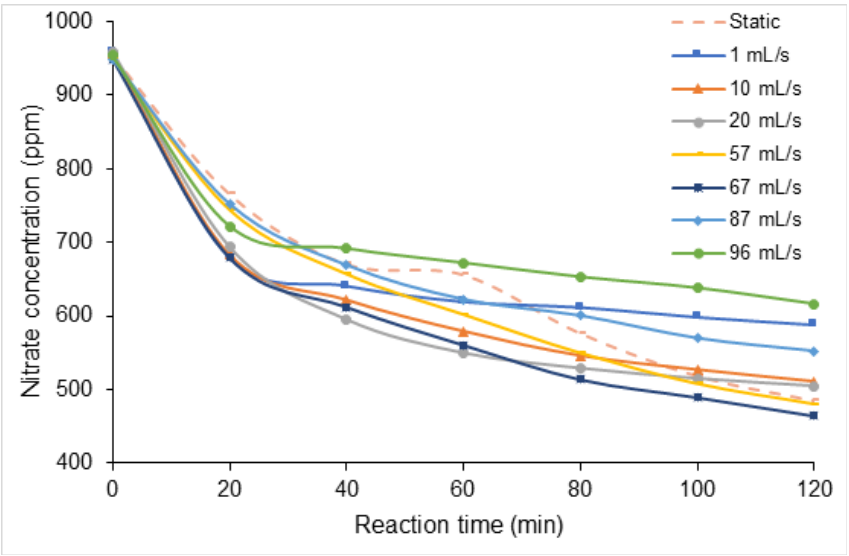

Figure 1: Flowrate effect on nitrate concentration during non-catalytic electroreduction in recycle mode. Volume of the reaction mixture = 1 L; [NO_3^-] = 1 g·L^{-1} (1000ppm) at intrinsic pH; Initial pH= 6.8. Inter-electrode distance: 4mm; Stainless steel electrode dimensions: 5cm x 5cm x 0.2cm.

Higher flow rate appears to be detrimental most likely due to short nitrate contact time within inter-electrodes space [25]. This result is of great importance, because it provides evidence of the beneficial effect of this partial recycle mode. One must also expect that full continuous flow should result in high process efficient., thereby justifying the approach tackled in the present work.

Effect of salts addition

The general tendency is that addition of all the salts investigated herein produced a significant improvement of nitrate electroreduction illustrated by marked concentration decay a significant improvement of nitrate electroreduction illustrated by a marked concentration decay as compared to the salt-free process (control experiment). Nitrate concentration dramatically dropped down to below 400 ppm in the presence of $MgCl_2$ after only 40min reaction and even below to ca. 146 and 115ppm after 120min for 1mL·s^{-1} and 37mL·s^{-1} flowrates, respectively (Figure 2). Similar effect but with a final nitrate concentration of 154ppm was registered for higher flow rate of 96mL/s (Figure S2).

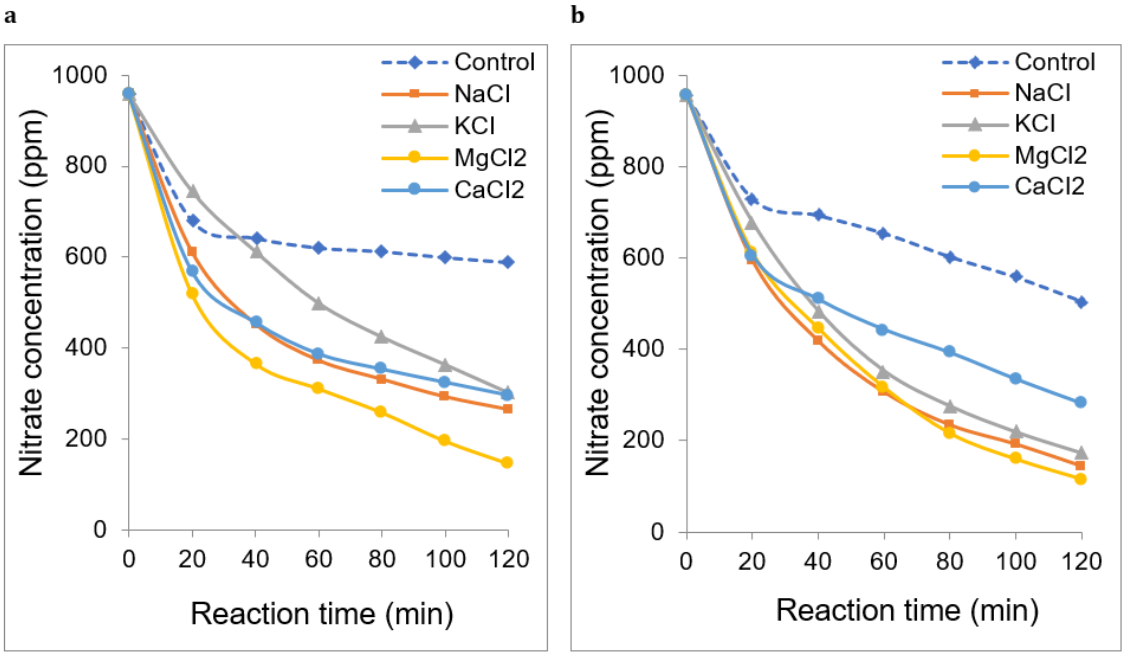

Figure 2: Effect of salt addition on non-catalytic nitrate electroreduction at different flowrates: a) 1mL·s^{-1}, b) 37mL·s^{-1}. Volume of the reaction mixture = 1L; [NO_3^-] = 1g·L^{-1} (1000ppm) at intrinsic pH; Salt concentration: 1000ppm at intrinsic pH; Stainless steel electrode dimensions: 5cm x 5cm x 0.2cm. Inter-electrode distance: 4mm; Voltage: 5V. The control experiment was achieved at the same throughput as in the absence of salt.

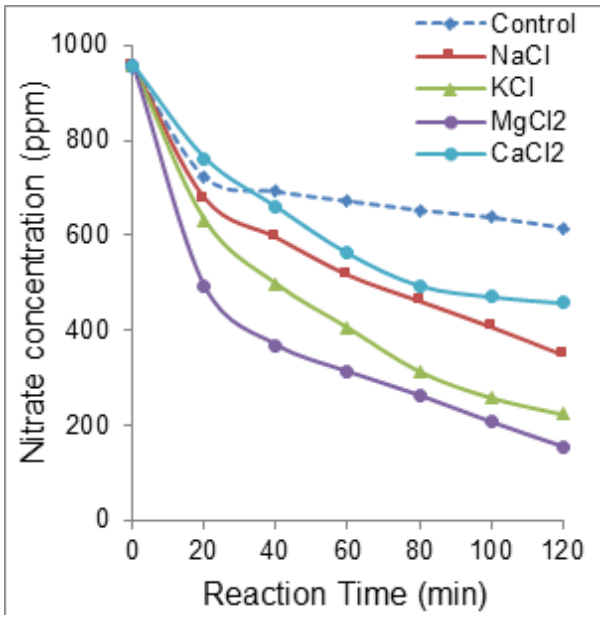

Figure S2: Effect of salt addition on nitrate electroreduction at 96mL·s^{-1} flow rate. Volume of the reaction mixture = 1L; [NO_3^-] = 1g·L^{-1} (1000ppm) at intrinsic pH; Salt concentration: 1000ppm at intrinsic pH; Stainless steel electrode dimensions: 5cm x 5cm x 0.2cm. Distance between electrodes: 4mm; Voltage: 5V.

The highest process enhancement was registered at a moderate 37mL·s^{-1} flowrate for all salts tested. This confirms this optimum throughput value for maximum nitrate electro-reduction according to our previous statement. Interestingly, the most pronounced decrease in nitration removal yields were registered for NaCl (65-86%) and $MgCl_2$ (85-88%) after 40min electroreduction (Table 1).

Ionic strength-liquid flowrate interdependence

Deeper insights in salt effect revealed that this must be due to the higher Ionic Strength (*IS*) of aqueous $MgCl_2$ and NaCl solutions (9.2x10^{-3} and 8.5x10^{-3} mol·L^{-1}, respectively) as compared to KCl (6.6.10^{-3}mol·L^{-1}) and $CaCl_2$ (3.5.10^{-3}mol·L^{-1}) (Table 1). This sequence was maintained after salt addition in the reaction mixture but with ca. 3 to 5 times higher IS values due to additional ion rise by both nitrate electroreduction and electrode corrosion.

For a given flowrate, this beneficial effect of the ionic strength is proportional to an improvement of the electric conductivity reflected by increased Current Density (*CD*) in agreement with the literature [13]. For instance, under a 37mL·s^{-1} flowrate, the highest nitrate conversion (88%) was registered for $MgCl_2$ and highest current density (50.9mA·cm^{-2}). Nevertheless, for the same cation, increasing the reaction mixture flowrate produced a visible decrease in the current density from 57.1mA·cm^{-2} under 1mL·s^{-1} to 50.9 and 44.9mA·cm^{-2} under slower flowrates. Therefore, it clearly appears that strong flowrates are detrimental because they reduce the contact time of ions in the inter-electrode space, thereby affecting the electrochemical process.

Surprisingly, under a flow rate of 96mL·s^{-1}, KCl displayed higher CD (58.5mA·cm^{-2}) than $MgCl_2$ (44.9mA·cm^{-2}) and NaCl (48.1mA·cm^{-2}). As expected, KCl produced lower nitrate electroreduction yield as compared to $MgCl_2$ (78 versus 86%) due to its lower IS value (22 versus 25 10^{-3}mol·L^{-1}, respectively). However, KCl gave a higher nitrate conversion yield than NaCl (78 versus 65%) in spite of its lower IS (22 versus 24 10^{-3}mol·L^{-1}). Thus, it clearly appears that even if the IS is a key-factor that determines nitrate conversion efficiency, the CD level and subsequently the reaction mixture flowrate seem to also play significant roles, and that a judicious approach should focus on an optimization of the *IS-CD* couple through an IS-flowrate correlation.

Effects of acid addition

Three series of experiments achieved in the absence of catalyst at different flow rates allowed investigating the effect of acid addition. A first overview of the results obtained revealed the beneficial effect of HCl addition and no clear process improvement with the other salts. Unlike the other salts, HCl addition produced the fastest and most pronounced nitrate depletion under weak flow rate of only 1mL·s^{-1} (Figure 3a).

Under stronger 37mL·s^{-1} (Figure 3b) and 96mL·s^{-1} flowrates (Figure S3), addition of all the investigated acids induced a clearer improvement of the electrochemical process reflected by low residual nitrate concentrations for all reaction times as compared to the acid-free reaction mixture. This improvement was slightly more pronounced for polyacids (H_2SO_4 and H_3PO^4). However, changes in the sequence of the acid efficiently were noticed for different flowrates, suggesting a strong interdependence between this parameter and the acid type.

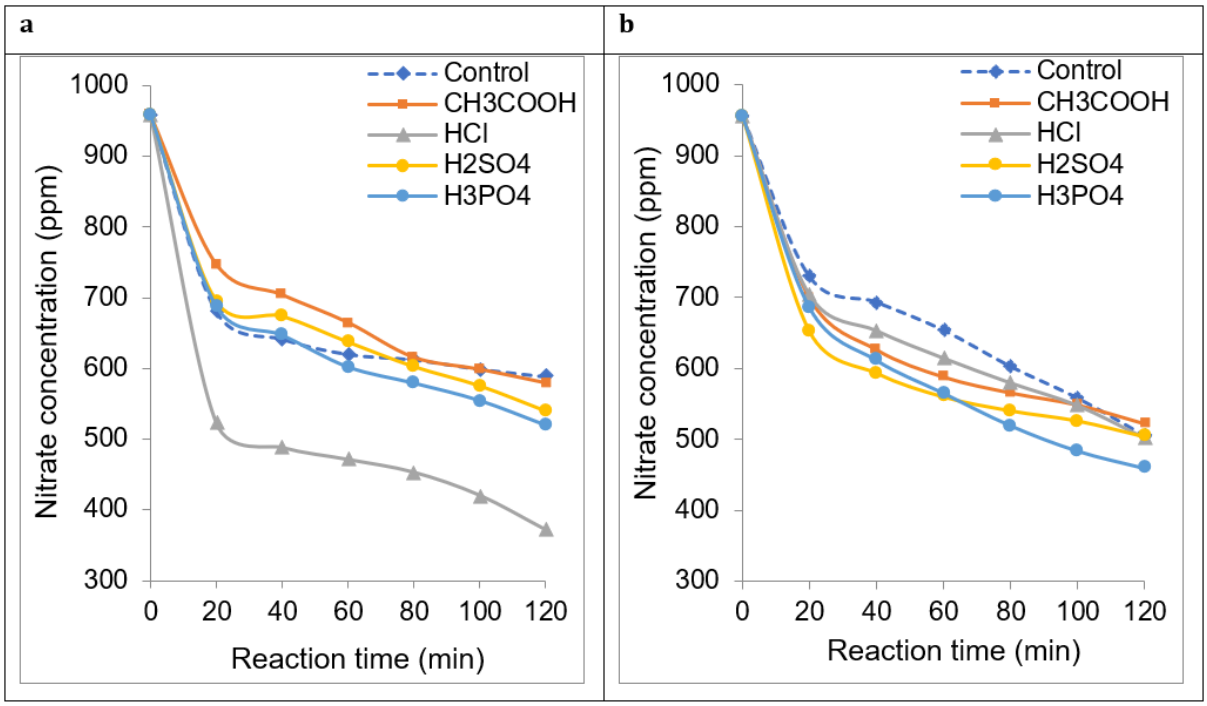

Figure 3: Effect of acid addition on non-catalytic nitrate electroreduction at different flows rates: a) 1mL·s^{-1}, b) 37mL·s^{-1}. Volume of the reaction mixture = 1L; [NO_3^-] = 1g·L^{-1} (1000ppm) at intrinsic pH; Salt concentration: 1000ppm at intrinsic pH; Stainless steel electrode dimensions: 5cm x 5cm x 0.2cm. Inter-electrode distance: 4mm; Voltage: 5V. The control experiment was achieved at the same throughput without adding acids.

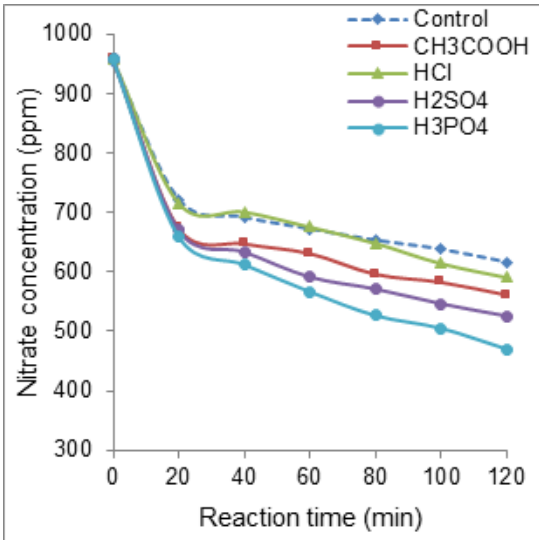

Figure S3: Effect of acid addition on non-catalytic nitrate electroreduction at a 96mL·s^{-1} throughput. Volume of the reaction mixture = 1L; [NO_3^-] = 1g·L^{-1} (1000ppm) at intrinsic pH; Salt concentration: 1000ppm at intrinsic pH; Stainless steel electrode dimensions: 5cm x 5cm x 0.2cm. Distance between electrodes: 4mm; Voltage: 5V.

Acid effect on ionic strength-liquid flowrate interdependence

Acid addition produced weaker improvement of the electroreduction process affording maximum conversion yield of 48-54% with a 37mL·s^{-1} flowrate versus 72-88% with salt addition (Table 1). Possible explanations may involve a stronger influence of salt addition and/or the occurrence of different optimum flowrate with acid addition. This was confirmed by deeper insights with various flowrates which revealed specific optimum flowrate within the range 40-80mL·s^{-1} for each added acid. Acetic and phosphoric acids gave maximum nitrate conversion yields of ca. 62% and to a lesser extent 53-54% for sulphuric after 120min of electrochemical process under a flowrate of approximately 75-76%mL·s^{-1} (Figure 4). Lower maximum conversion yield of 55% was obtained with HCl under 60-70mL·s^{-1} flowrate after 120min of non-catalytic nitrate electro-reduction of up 63% under a 1mL·s^{-1} flowrate.

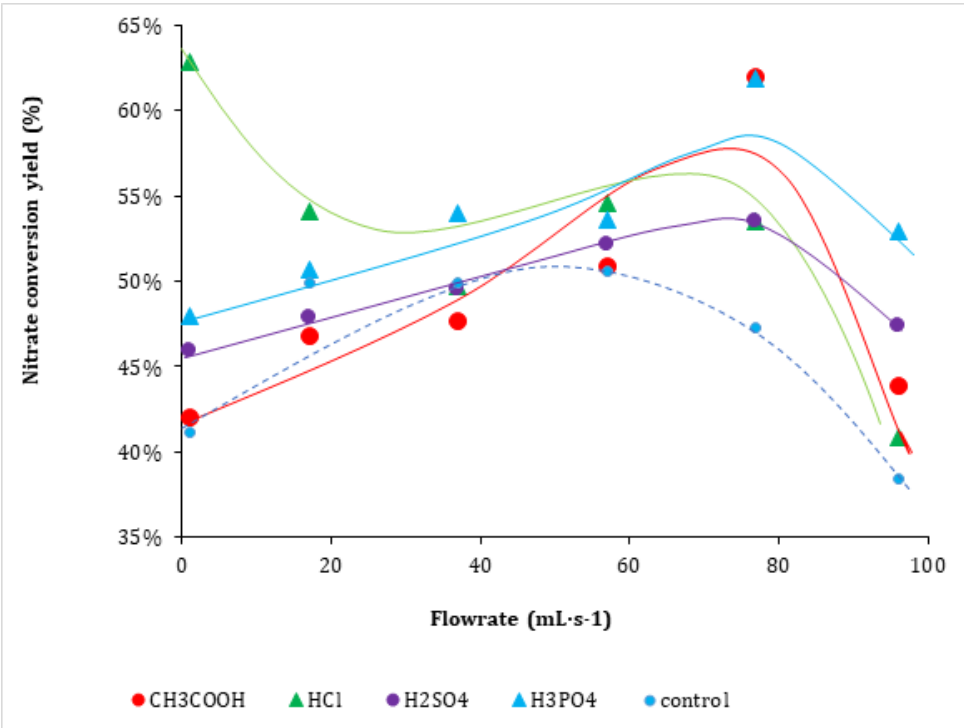

Figure 4: Effect of the flow rate on non-catalytic nitrate electro-reduction yield after 120 minutes: a) 1mL·s^{-1}, b) 37mL·s^{-1} and c) 96mL·s^{-1}. Volume of the reaction mixture = 1L; [NO_3^-] = 1g·L^{-1} (1000ppm) at intrinsic pH; Salt concentration: 1000ppm at intrinsic pH; Stainless steel electrode dimensions: 5cm x 5cm x 0.2cm. Inter-electrode distance: 4mm; Voltage: 5V.

Table 1: Effect of salt addition on current density and ionic strength under different flow rates.

Reaction time: 40min. Volume of the reaction mixture = 1L; [NO_3^-] = 1g·L^{-1} (1000ppm) at intrinsic pH; Salt concentration: 1000ppm at intrinsic pH; Stainless steel electrode dimensions: 5cm x 5cm x 0.2cm. Inter-electrode distance: 4mm; Voltage: 5V.

*The aqueous reaction mixture displays a total ionic strength (IS) before (a) after nitrate electroduction (b).

Added Species		Final Yield (%)			Current Density (mA·cm^{-2})			Salt Ionic Strength (10^{-3}mol·L^{-1})	
		Flowrate (mL·s^{-1})			Flowrate (mL·s^{-1})				
		1	37	96	1	37	96	t_o=0	t=40min
Salts	$MgCl_2.6H_2O$	85	88	85	57.6	50.9	44.9	9.2	25
	NaCl	74	86	65	57.1	53.6	48.1	8.5	24
	KCl	70	83	78	41.5	50.6	58.5	6.6	22
	$CaCl_2.2H_2O$	70	72	54	34.8	34.7	27.0	3.5	19
Control:	**None**	**41**	**43**	**38**	**33.4**	**23.9**	**17.6**	**-**	**16**
Acids	H_3PO_4	42	48	44	32.1	31.7	30.8	45	61
	H_2SO_4	46	50	47	18.9	19.8	18.8	20	36
	HCl	63	50	41	18.1	19.1	21.3	14	30
	CH_3COOH	48	54	53	29.9	31.4	30.2	8	24

All acids added induced a significant IS increase but slight to barely detectable CD decrease with increasing flowrate from 1 to 96mL·s^{-1} (Table 1). However, unlike both polyacids added (H_2SO_4 and H_3PO_4), HCl and acetic acid produced visible CD increase from 18.1 to 21.3mA·cm^{-2}. It is worth mentioning that the higher IS values (24-61x10^{-3}mol·L^{-1}) induced by acid addition as compared to salt addition (19-25x10^{-3}mol·L^{-1}) resulted in a shift of the optimum flowrate from moderate 37mL·s^{-1} towards higher values in the range 40-80mL·s^{-1} . This also produced lower CD levels that explain the weaker nitration conversion yields. This result is also of a great importance because it clearly demonstrates that the IS-flowrate independence is unavoidably governed by the acid addition and type of acid added.

Acid addition turned out to be beneficial only for flow rates exceeding 60mL·s^{-1}, providing evidence that H^+ ion play a key-role in the electrochemical process. This effect of proton was somehow expected because this species is supposed to reduce the detrimental effect of the formation of hydroxyl anion by most reactions including the main reaction of nitrate reduction into nitrogen (2 NO_3^- + 6 H_2O + 10 $e^- \rightarrow N_2$ + 12 OH^-). Nevetheless, excessive proton concentration must alter the electrodes, unlike moderately acidic species. The latter are supposed to improve nitrate electroreduction by increasing the ion current density as already reported [28], and to favor the ion mobility in the solution without electrode alteration by acid attack [28,45]. Research is still in progress in this direction.

Catalyst-flowrate interdependence

Almost similar evolution in time of nitrate conversion was noticed with all catalysts within the investigated flowrate range (Figure 5 & Figure S4). The nitrate electroreduction yield dropped from 588-615ppm after 120min of non-catalytic process down to 528 and 429ppm under 1 and 37mL·s^{-1} flowrate, respectively after addition of an illite-montmorillonite mixture ((I+M). The latter showed the highest catalytic activity as illustrated by lowest residual nitrate concentration after 120min of catalytic process. Here also, the sequence of catalyst performances appears to change according to the flowrate, since the Kaolin-type clay material gave a lower residual nitrate concentration (452ppm) as compared to I+M (527ppm) under a 96mL·s^{-1} flowrate (Figure S4). Under these conditions, all catalysts produced an improvement of the electrochemical process affording lower residual nitrate concentration after 120min process unlike under lower flowrates.

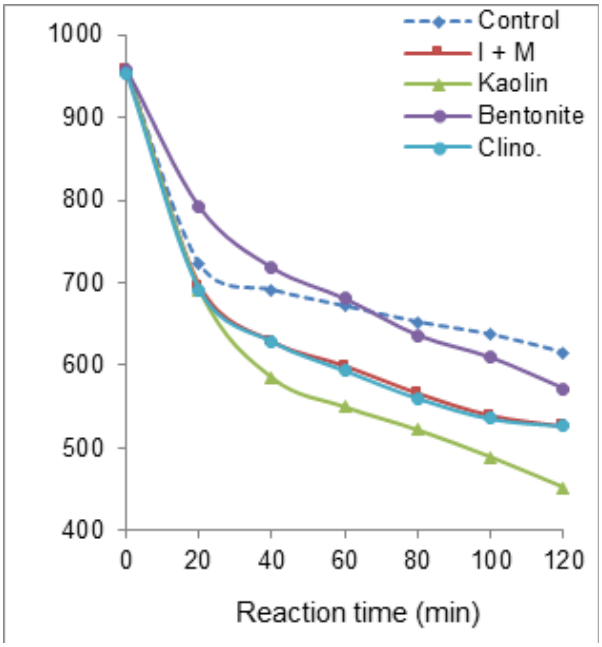

Figure S4: Effect of catalyst addition on the evolution in time of nitrate concentration under 96mL·s^{-1} flow rate. Volume of the reaction mixture = 1L; [NO_3^-] = 1g·L^{-1} (1000ppm) at intrinsic pH; Salt concentration: 1000ppm at intrinsic pH; Stainless steel electrode dimensions: 5cm x 5cm x 0.2cm. Inter-electrode distance: 4mm; Voltage: 5V. Catalyst concentration:0.2g.L^{-1}. The control experiment achieved at the same throughput in the absence of catalyst.

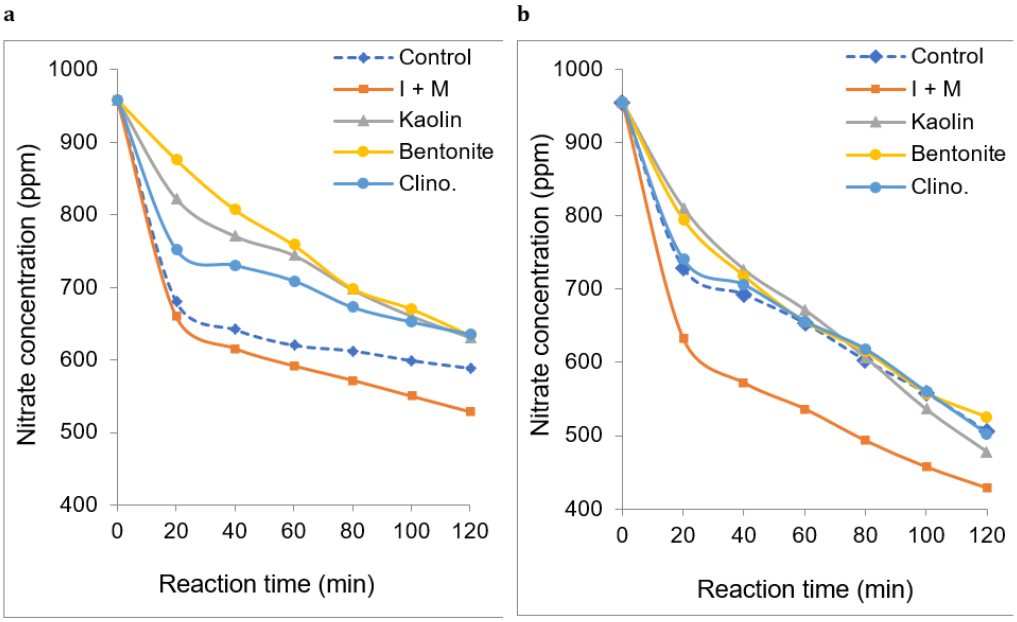

Figure 5: Effect of catalyst addition on the evolution in time of nitrate concentration under 1mL·s^{-1} (a) and 37mL·s^{-1} (b) flow rate. Volume of the reaction mixture = 1L; [NO_3^-] = 1g·L^{-1} (1000ppm) at intrinsic pH; Salt concentration: 1000ppm at intrinsic pH; Stainless steel electrode dimensions: 5cm x 5cm x 0.2cm. Inter-electrode distance: 4mm; Voltage: 5V. Catalyst concentration: 0.2g.L^{-1}. The control experiment was achieved at the same throughput in the absence of catalyst.

There exists a narrow catalyst-flowrate interdependence, since kaolin and to a lesser extent clinoptilolite and I+M mixture exhibited the highest nitrate conversion levels at high flow rate. Notwithstanding that native crude bentonite is the most convenient catalyst without purification, this material turned out to fairly non-effective affording similar or even lower nitrate removal than the very absence of solid catalysts for low flowrate below 55-56mL·s^{-1} after 120 minutes of catalytic electroreduction (Figure 5).

Bentonite, clinoptilolite and kaolin gave maximum nitrate conversion yields of ca. 55, 58 and 59% around an optimum 75-78mL·s^{-1} flowrate. I+M mixture showed higher maximum nitrate conversion yield of ca. 62-63% at lower flow rate of 55-57mL·s^{-1}. The higher effectiveness of 1:1 wt./wt. illite-montmorillonite mixture can be explained by the role of an optimum density of charge surface. [I+M] mixture is expected to display an intermediate Cation Exchange Capacity (CEC) comprised between, on one hand, those of bentonite and pure montmorillonite (70-100meq/100g) and, on the other hand, those of illite (25-40meq/100g) and kaolinite (3-15meq/100g) (Figure 6).

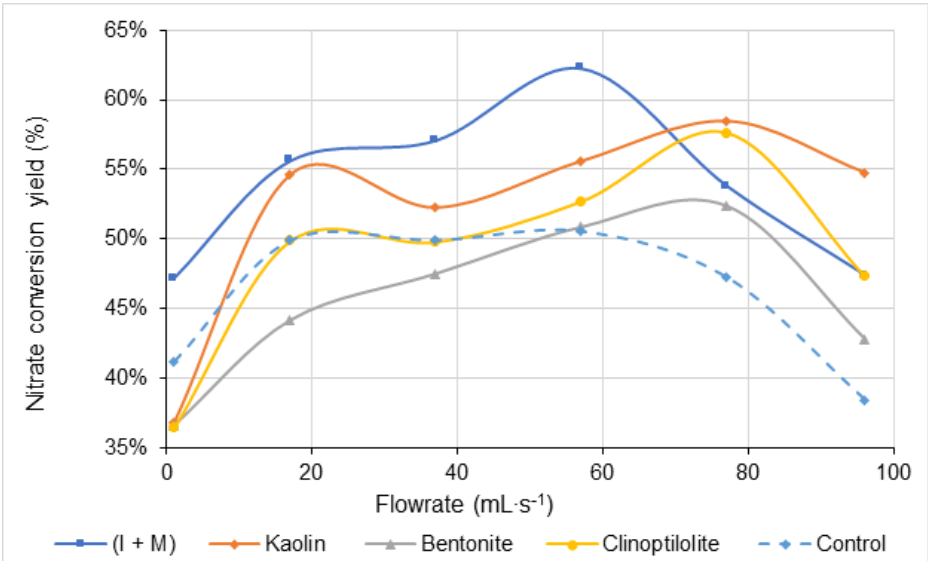

Figure 6: Flow rate effect on nitrate conversion yield after 120 minutes of catalytic electroreduction. Volume of the reaction mixture = 1L; [NO_3^-] = 1g·L^{-1} (1000ppm) at intrinsic pH; Salt concentration: 1000ppm at intrinsic pH; Stainless steel electrode dimensions: 5cm x 5cm x 0.2cm. Inter-electrode distance: 4mm; Voltage: 5V. The control experiment was achieved at the same throughput in the absence of catalyst.

On clay mineral surfaces, increasing CEC should improve the electrostatic forces that are strongly required for both nitrate adsorption and surface catalytic reaction. These forces are expected to be proportional to the catalyst surface and subsequently to the dispersion grade of the clay particles. Optimum surface charges induce optimum surface electrostatic forces, because excessive surface charges cause particle aggregation through coagulation-flocculation [46,47]. This is supposed to hinder nitrate adsorption and surface reaction. Besides, the beneficial effect of acid addition suggests that the higher catalytic activity of the I+M mixture as compared to the other aluminosilicates may be due to its higher surface acidity. This increased acidity should be proportional to the higher Si/Al ratio [43,48]. The latter is supposed to be comprised between those of crude bentonite and pure Illite [13]. Therefore, the I+M mixture showed the highest nitrate removal yield, at least under low to moderate flowrate. The lack of clear correlation with the Si/Al ratio and catalytic activity of aluminosilicates must be due to shading effects of the pH-dependent aluminosilicate dispersion in aqueous media and interaction with other species.

Conclusion

The results obtained herein allow concluding that flowrate variation improves nitrate electro-reduction but only up to a certain level. Nitrate conversion of up to 88% was achieved when adding $MgCl_2$ for a 37mL.s^{-1} throughput without precipitation upon alkalinity increase in time. Chlorinated salts appear to promote the electrochemical denitrification rate through enhancements of the ionic strength and current density. Illite-Montmorillonite gave highest nitrate conversion due to their optimum CEC. The beneficial effect of acid addition in non-catalytic nitrate electroreduction appears to rather be due to much higher ionic strength as compared to salt addition. An almost reverse proportionality was noticed between the process efficiency and acid strength, since weak acid gave highest nitrate conversion yields and ionic forces. This is explained in terms of electrode alteration by acid attack in the presence of strong acids. Deeper insights in the combined effects of the investigated factors will certainly provide valuable data for prospective clay-catalyzed water treatment technologies. These results already open promising prospects for silica-rich materials for effective electro-catalytic nitrate removal in dynamic conditions.

References

1. Ferreira JG, Bricker SB, Simas TC (2007) Application and sensitivity testing of a eutrophication assessment method on coastal systems in the United States and European Union. Journal of Environmental Management 82(4): 433-445.
2. Lord EI, Anthony SG, Goodlass G (2002) Agricultural nitrogen balance and water quality in the UK. Soil Use and Management 18(4): 363-369.
3. Schröder JJ, Scholefield D, Cabral F, Hofman G (2004) The effects of nutrient losses from agriculture on ground and surface water quality: the position of science in developing indicators for regulation. Environmental Science & Policy 7(1): 15-23.
4. Liu A, Ming J, Ankumah RO (2005) Nitrate contamination in private wells in rural Alabama, United States. Science of the Total Environment 346(1-3): 112-120.
5. Fewtrell L (2004) Drinking-water nitrate, methemoglobinemia, and global burden of disease: A discussion. Environmental Health Perspectives 112(14): 1371-1374.
6. Esmaeili A, Moore F, Keshavarzi B (2014) Nitrate contamination in irrigation groundwater, Isfahan, Iran. Environmental Earth Sciences 72(7): 2511-2522.
7. Siripong S, Rittmann BE (2007) Diversity study of nitrifying bacteria in full-scale municipal wastewater treatment plants. Water Research 41(5): 1110-1120.
8. Wang J, Chu L (2016) Biological nitrate removal from water and wastewater by solid-phase denitrification process. Biotechnology Advances 34(6): 1103-1112.
9. Banu HT, Meenakshi S (2017) Synthesis of a novel quaternized form of melamine--formaldehyde resin for the removal of nitrate from water. Journal of Water Process Engineering 16(Supplement C): 81-89.
10. Desjardins R (1997) Water treatment (2nd edn).
11. Kapoor A, Viraraghavan T (1997) Nitrate removal from drinking water-Review. Journal of Environmental Engineering 123(4): 371-380.
12. Talhi B, Monette F, Azzouz A (2011) Effective and selective nitrate electroreduction into nitrogen through synergistic parameter interactions. Electrochimica Acta 58: 276-284.
13. Enmili A, Azzouz A, Vasilica-Alisa A, Monette F (2016) Aluminosilicate-catalyzed electroreduction of nitrate anion-An approach through alkalinity analysis. Electrochimica Acta 222: 1064-1071.
14. Paidar M, Roušar I, Bouzek K (1999) Electrochemical removal of nitrate ions in waste solutions after regeneration of ion exchange columns. Journal of Applied Electrochemistry 29(5): 611-617.
15. Hsieh SJ, Gewirth AA (2000) Nitrate reduction catalyzed by underpotentially deposited Cd on Au (111): Identification of the electroactive surface structure. Langmuir 16(24): 9501-9512.
16. Ding J (2015) Electroreduction of nitrate in water: Role of cathode and cell configuration. Chemical Engineering Journal 271: 252-259.
17. Dima GE, de Vooys ACA, Koper MTM (2003) Electrocatalytic reduction of nitrate at low concentration on coinage and transition-metal electrodes in acid solutions. Journal of Electroanalytical Chemistry 554-555: 15-23.
18. Reyter D, Bélanger D, Roué L (2008) Study of the electroreduction of nitrate on copper in alkaline solution. Electrochimica Acta 53(20): 5977-5984.
19. Katsounaros I, Kyriacou G (2008) Influence of nitrate concentration on its electrochemical reduction on tin cathode: Identification of reaction intermediates. Electrochimica Acta 53(17): 5477-5484.
20. Bouzek K, Paidar M, Sadílková A, Bergmann H (2001) Electrochemical reduction of nitrate in weakly alkaline solutions. Journal of Applied Electrochemistry 31(11): 1185-1193.
21. Dash BP, Chaudhari S (2005) Electrochemical denitrificaton of simulated ground water. Water Research 39(17): 4065-4072.
22. Govindan K, Noel M, Mohan R (2015) Removal of nitrate ion from water by electrochemical approaches. Journal of Water Process Engineering 6: 58-63.
23. Lacasa E (2012) Effect of the cathode material on the removal of nitrates by electrolysis in non-chloride media. Journal of Hazardous Materials 213(Supplement C): 478-484.
24. Mácová Z, Bouzek K, Šerák J (2007) Electrocatalytic activity of copper alloys for NO_3 - reduction in a weakly alkaline solution. Journal of Applied Electrochemistry 37(5): 557-566.
25. Reyter D, Bélanger D, Roué L (2011) Optimization of the cathode material for nitrate removal by a paired electrolysis process. Journal of Hazardous Materials 192(2): 507-513.
26. Polatides C, Kyriacou G (2005) Electrochemical reduction of nitrate ion on various cathodes - reaction kinetics on bronze cathode. Journal of Applied Electrochemistry 35(5): 421-427.
27. Szpyrkowicz L (2006) Removal of NO_3- from water by electrochemical

reduction in different reactor configurations. Applied Catalysis B: Environmental 66(1): 40-50.

28. de Vooys ACA, van Santen RA, van Veen JAR (2000) Electrocatalytic reduction of NO_3- on palladium/copper electrodes. Journal of Molecular Catalysis A: Chemical 154(1-2): 203-215.

29. Zöllig H, Morgenroth E, Udert KM (2015) Inhibition of direct electrolytic ammonia oxidation due to a change in local pH. Electrochimica Acta 165: 348-355.

30. Zöllig H, Fritzsche C, Morgenroth E, Udert KM (2015) Direct electrochemical oxidation of ammonia on graphite as a treatment option for stored source-separated urine. Water Research 69: 284-294.

31. Enmili A (2020) Aluminosilicate-catalyzed electrochemical removal of ammonium cation from water-kinetics and selectivity. Environmental Research 185: 109412.

32. Li L, Liu Y (2009) Ammonia removal in electrochemical oxidation: Mechanism and pseudo-kinetics. Journal of Hazardous Materials 161(2): 1010-1016.

33. Wasmus S (1994) DEMS-cyclic voltammetry investigation of the electrochemistry of nitrogen compounds in 0.5 M potassium hydroxide. Electrochimica Acta 39(1): 23-31.

34. Gootzen JFE (1998) A DEMS and cyclic voltammetry study of NH3 oxidation on platinized platinum. Electrochimica Acta 43(12): 1851-1861.

35. de Vooys ACA, Koper MTM, van Santen RA, van Veen JAR (2001) The role of adsorbates in the electrochemical oxidation of ammonia on noble and transition metal electrodes. Journal of Electroanalytical Chemistry 506(2): 127-137.

36. American Public Health A (2005) Standard methods for the examination of water and wastewater. Washington DC, USA.

37. Azzouz A, Nistor D, Miron D, Ursu AV, Sajin T, et al. (2006) Assessment of acid–base strength distribution of ion-exchanged montmorillonites through NH_3 and CO_2-TPD measurements. Thermochimica Acta 449(1-2): 27-34.

38. Bieseki L, Bertell F, Treichel H, Penha FG, Pergher SBC (2013) Acid treatments of montmorillonite-rich clay for Fe removal using a factorial design method. Materials Research 16(5): 1122-1127.

39. Didi M (2002) NMR Study of the action of phosphorus pentoxide on p-(1,1,3,3-tetramethylbutyl) phenol. pp. 631-639.

40. Didi MA, Makhoukhi B, Azzouz A, Villemin D (2009) Colza oil bleaching through optimized acid activation of bentonite. A comparative study. Applied Clay Science 42(3): 336-344.

41. Dumitriu E (1999) Synthesis optimization of chabasite-like SAPO-47 in the presence of sec-butylamine. Microporous and Mesoporous Materials 31(1): 187-193.

42. Larouk S, Ouargli R, Shahidi D, Olhund L, Shiao TC (2017) Catalytic ozonation of orange-G through highly interactive contributions of hematite and SBA-16 - To better understand azo-dye oxidation in nature. Chemosphere 168: 1648-1657.

43. Makhoukhi B (2009) Acid activation of Bentonite for use as a vegetable oil bleaching agent. Fats and oils 60(4): 343-349.

44. Shahidi D, Roy R, Azzouz A (2014) Total removal of oxalic acid via synergistic parameter interaction in montmorillonite catalyzed ozonation. Journal of Environmental Chemical Engineering 2(1): 20-30.

45. Safonova TY, Petrii OA (1998) Effect of inorganic cations on the electroreduction of nitrate anions on Pt|Pt electrodes in sulfuric acid solutions. Journal of Electroanalytical Chemistry 448(2): 211-216.

46. Assaad E, Azzouz A, Nistor D, Ursu AV, Sajin T, et al. (2007) Metal removal through synergic coagulation–flocculation using an optimized chitosan-montmorillonite system. Applied Clay Science 37(3-4): 258-274.

47. Azzouz A (2009) Chitosan-colloidal particle interactions. Synergy with clays. in Chitin and chitosan (from biopolymer to application).

48. Arus VA, Nousir S, Sennour R, Shiao TC Nistor ID, et al. (2018) Intrinsic affinity of acid-activated bentonite towards hydrogen and carbon dioxide. International Journal of Hydrogen Energy 43(16): 7964-7972.